Cement and Concrete Research 39 (2009) 997–1006

Contents lists available at ScienceDirect

Cement and Concrete Research

journal homepage: http://ees.elsevier.com/CEMCON/default.asp

Flow conditions of fresh mortar and concrete in different pipes

Stefan Jacobsen [a,*], Lars Haugan [b], Tor Arne Hammer [b], Evangelos Kalogiannidis [a]

[a] Norwegian University of Science and Technology, Dept of Structural Engineering, Trondheim, Norway
[b] SINTEF Byggforsk AS Building and Infrastructure, Trondheim, Norway

ARTICLE INFO

Article history:
Received 24 February 2009
Accepted 10 July 2009

Keywords:
Fresh concrete
Workability
Rheology
Pumping

ABSTRACT

The variation in fresh concrete flow rate over the pipe cross section was investigated on differently coloured and highly flowable concrete mixes flowing through pipes of different materials (rubber, steel, acryl). First, uncoloured (gray) concrete was poured through the pipe and the pipe blocked. Similar but coloured (black) concrete was then poured into the pipe filled with gray concrete, flowing after the gray concrete for a while before being blocked and hardened. The advance of the colouring along the pipe wall (showing boundary flow rate) was observed on the moulded concrete surface appearing after removing the pipe from the hardened concrete. The shapes of the interfaces between uncoloured and coloured concrete (showing variation of flow rate over the pipe cross section) were observed on sawn surfaces of concrete half cylinders cut along the length axes of the concrete-filled pipe. Flow profiles over the pipe cross section were clearly seen with maximum flow rates near the centre of the pipe and low flow rate at the pipe wall (typically rubber pipe with reference concrete without silica fume and/or stabilizers). More plug-shaped profiles, with long slip layers and less variation of flow rate over the cross section, were also seen (typically in smooth acrylic pipes). Flow rate, amount of concrete sticking to the wall after flow and SEM-images of pipe surface roughness were observed, illustrating the problem of testing full scale pumping.

1. Introduction

Pumpability is mainly depending on the fresh concrete, but cannot only be defined in terms of rheological properties. Since pumping concrete is a widely used method for distribution and placement due to the increasing need for speedy construction [1,2] the pumpability is of practical importance for the industry. Both fundamental parameters governing flow and placement of concrete [3–6] and hardened properties are included in the practical definition of concrete pumpability; "ability to flow through pipes and hoses by the help of a pump without negative effect on fresh and hardened properties" [7,8]. The main parameters of pumpability have been reviewed and studied [1,2,9–11] and can be divided into site conditions (type of pump, size, length and material of pipe, energy use, required flow etc) and concrete technology (composition, rheology, age etc).

To predict pumpability of a certain concrete mix in a specific pumping set-up, the complex relation between concrete rheology and pumpability needs elucidation. In addition there are various physical phenomena involved. In [1,12,13] two different flow mechanisms were proposed; plug/slip- and/or shear flow. Equipment, concrete composition and rheology affect both these two flow modes. The plug/slip action is assumed to be facilitated by a slip layer between the concrete and the pipe wall. Prior to pumping, the slip layer is usually established by pipeline priming, but during successful pumping it is probably maintained by the concrete. The concrete should neither have too low nor too high fines content depending on aggregate packing, size, shape etc. Furthermore, there should neither be too much nor too fast pressurized bleeding to avoid a dewatered plug, nor too high friction at the pipe wall. The shear conditions of the bulk flow motion can be assumed to depend on whether the concrete yield stress is surpassed. The yield stress can be assumed to be reached first near the wall, and the plug radius reduced towards the centre of the pipe at increasing pressure [10]. For such shear flow development, plastic viscosity governs the velocity profile between the moving plug and the pipe wall, as flow and shear rate increase and the plug eventually disappears if the resulting shear action on the surface of the plug surpasses the yield stress over the whole cross section. This is quantified by Eq. (1) below.

Few experimental studies on the relation between rheology and pumpability exist. In a study on the relation between concrete rheology and hydraulic oil pressure in a piston pump at 200 m vertical concrete pumping during the production of a North sea off-shore structure [14], measurements were made with the MkII viscometer [10,15] before and after pumping. The results showed that both the yield, g (Nm), and the rate of change, h (Nms), related to the pressure. Best relation was found between increasing yield and increased pressure. Also slump was measured, and related best to reduced pressure. The investigated concrete mixes had w/b = 0.42–0.45, 420 kg of cement, 2% silica fume, around 1.2% superplasticizer by weight of cement and 190–240 mm slump. A more complete study was made on a French construction site [16], measuring fresh concrete

* Corresponding author.
E-mail address: stefan.jacobsen@ntnu.no (S. Jacobsen).

0008-8846/$ – see front matter
doi:10.1016/j.cemconres.2009.07.005

line pressure, -flow and plastic viscosity, μ (Pa·s), and yield stress, τ_0 (Pa), in the BTRHEOM viscometer [15] on a range of concretes pumped with piston pumps. Flow, v (m/s), through a pipe can be calculated with the Buckingham–Reiner equation, Eq. (1), relating pressure, flow and rheology for laminar flow in a Bingham fluid (like Hagen–Poiseuille's equation does for a Newtonian fluid) [9,10,16]:

$$v = \frac{\pi r^2}{8\mu}\frac{dp}{dx}\left[1-4\left(\frac{R_0}{3r}\right)+\left(\frac{R_0}{3r}\right)^4\right]. \quad (1)$$

Here, dp/dx (Pa/m) is pressure gradient over the pump line, R_0 (m) is plug radius, r (m) is pipe radius and μ (Pa s) plastic viscosity. The plug radius is derived from mechanical equilibrium of the plug in the pipe axis giving Eq. (2):

$$R_0 = 2\tau_0\frac{dp}{dx}. \quad (2)$$

Here, the yield, τ_0 (Pa), is that of the concrete in the plug. It was found that Eq. (1) always predicted too low flow compared to measured pipe line flow for the concretes [16]. Therefore, a surface slip/tribology test was later developed, giving improved pump flow prediction with a new slip layer viscosity model [2]. In [11], pumping experiments were made on a wide range of concretes and mortars with τ_0 and μ ranging from almost zero to around 800 Pa and 100 Pa s respectively, slump values in the range of 60 to 240 mm and slump flow in the range of 400–900 mm. τ_0 and μ were measured with the BML viscometer [15,17–20]. All materials in [11] were pumped through 30 or 50 mm diameter rubber hoses of up to 70 m length using screw pump and measuring v and dp/dx. The same underestimation of Eq. (1) was observed as with the piston pump in [16]. Visual appearance of the fresh materials at the hose end varied from stiff, sometimes with a visible wet surface on the exiting plug, to highly flowing, almost liquid like. Calculated R_0, based on measured pump line pressure and yield (BML viscometer), varied from around 10 times the actual hose diameter to practically zero. This was in line with the visually observed plug-like or liquid-like appearance of the output material. Reynolds numbers varied from <1 to almost 100, also indicating possibilities for a wide spectre of flow conditions from plug to viscous flow of some kind.

Direct observations of flow profiles can increase our understanding of how concrete flows in pipes. Such observations are unfortunately rather few. Two early experimental studies of flow characteristics of concrete during pumping used coloured concrete pumped into pipes filled with uncoloured (gray) concrete [9,21]. Interfaces on sawn concrete cross sections were observed after hardening in the pipes. In [21], the visual observations showed both the existence of flow velocity profiles and porous, paste rich zones at the pipe wall, indicating a water rich slip layer as well as shear action over the cross section. In addition, orientation tendencies of aggregate particles were observed [21]. No details about concrete or pumping characteristics were given. In [9], coloured, stiff plastic consistency concrete mixes flowed into uncoloured mixes and were then left to harden in the steel pipes. Sections were sawn in the longitudinal and transversal direction of the 125 mm diameter pipes showing clear profiles and slip layers of plastic consistency concrete. Coloured concrete can also be used to observe flow during form filling. In [3], coloured self compacting concrete was pumped into gray concrete, revealing some of the flow patterns from observations of coloured concrete on the concrete surface after form work removal. In [22], transparent polymer matrix mixes with variable viscosity containing aggregate particles were observed through transparent acryl ("plexiglass") during flow. The aggregate particles were either smooth plastic balls or LWA particles with a bit rougher surface. The forward increase of coarse aggregate particle concentration was most sensitive to matrix viscosity for the LWA particles. The LWA particles resulted in higher forward particle content at low than at high matrix viscosity. Blockage occurred by arch formation of the roughest particles, particularly at tapering. Studies of hardened blocked concrete in pipes after full scale piston pumping [2,23] showed that coarse aggregate particles pressed together formed the blocking. The authors proposed the blocking mechanism as forward segregation, due to the acceleration of these large particles in a paste or matrix with too low viscosity during the stroke of piston pumps. An expression was derived combining Stokes law and Newton's second law, giving a differential equation found to fit reasonably [2,23] to the observed coarse aggregate movement up to the observed blocking. The same authors also applied fast measurements of bleeding rate, correlating just as well to pumpability and blocking tendency as the more tedious pressurized bleeding and slump measurements recommended in [13] did. The two negative effects on pumpability, coarse aggregate segregation and pressurized bleeding, were thus bridged [23].

Additional useful information with coloured fresh concrete was obtained in an experiment with colouring agent injected in the fresh concrete along the inner, static cylinder of the BML viscometer [24]. The colouring agent stayed at the static core of the concentric viscometer during rotation. This indicates that whatever flow conditions (shear, plug/slip), the lowest pressure occurred at the interface to the static steel core, and/or that the colouring stayed in the lubricating layer, not spreading into the fresh concrete.

Despite the above discussion, it seems that viscometry cannot predict pumpability unambiguously. There is therefore a need for direct visualisation of the flow conditions of modern types of highly flow able concrete: slip layer existence and/or movement, and existence of plug or flow profiles. The scope of the experimental part of this work is therefore to investigate whether coloured concrete can be used to observe variation of flow rate over a cross section and existence and/or nature of slip layers in modern highly flow able concrete. The experimental setup is based on the investigations [9,21] with observations of flow profiles on sawn surfaces, but modified to include surface observations of the colouring to indicate movement of the slip layer during gravitational flow. For this purpose coloured fresh concrete was poured into pipes just filled with similar uncoloured fresh concrete, and both concretes let flowing together for a while before blocking the pipe. Different pipe materials were studied, flow rate and amount of concrete sticking to the pipe measured, and observations made of pipe surface roughness by SEM.

2. Experiments

2.1. Flow test

A pilot study was first conducted. There, two mortars with flowing consistency, one without and one with colouring agent were poured through straight observation pipes. These were 30 mm inner diameter and 60 cm long PVC pipes kept at varying angles with the horizontal plane; 0, 15, 30, 45 and 90°. The observation pipes had sliding plates going through slots cut normally to the length axis at both ends for shutting. First, uncoloured mortar was filled via a funnel mounted on top of a 25 cm long vertical pipe leading down to the observation pipe that was fixed to a stand and shut at the lower end. Then the funnel and the vertical pipe were emptied and remounted. Finally, the observation pipe was partly filled with coloured mortar by letting out half a litre of gray mortar at the lower end by first opening the upper and then the lower shutter. The time to fill half a litre of mortar into a beaker was noted. Then, both ends of the observation pipe were shut and it was left to harden for 4 days.

Following experiences with the pilot study, a larger test set-up was made for more accurate simultaneous flow measurements, inspired by [25,26]. Three different types of pipes were investigated; acrylic ("plexiglass") and rubber with 45 mm, and steel pipes with 40 mm inner diameter. The observation pipes were all tilted at 45° to the horizontal plane, see Fig. 1. The height of the vertical filling pipes leading down to the observation pipe were now increased to 1.75 m with a

Fig. 1. Experimental set-up Mixes 1–4.

Fig. 2. Filling with coloured concrete.

funnel on top, and the observation sections were 1.1 m long. The same types of shutting plates at the ends of the observation pipe were used. First the two pipes were mounted and filled with uncoloured concrete, see Fig. 2. Flow was measured while approximately 6 kg of concrete was flowing into a beaker on a scale, registering the flow by logging weight and time. This kind of weighing procedure has given good reproducibility in similar tests of matrix flow resistance [25]. Then the upper end of the observation pipe was shut while filled with gray concrete. The vertical pipe was emptied, re-connected and filled with readily prepared coloured fresh concrete. The upper shutter was removed so that coloured concrete could flow into the observation pipe as the lower shutter was opened. Then, around 1 l of gray concrete was let out from the observation pipe, filling it approximately halfway with coloured concrete before the lower and then the upper shutters were closed. The observation pipe was left carefully to harden for 3–4 days. Then it was cut with diamond blade along the central axis to display the flow profile between uncoloured and coloured concrete. Finally, the pipe was removed to display the progress of the colouring along the surface of the concrete facing the pipe wall.

2.2. Concrete materials and mixtures

A number of trial mixes were made to obtain highly flowing, practically self compacting concrete that could flow through the pipes under its own weight and yet be stable against separation or excess bleeding. The mixes were prepared in a 10 l flat bottomed, horizontally rotating counter current mixer with two paddles. Dry materials were mixed for 1 min before admixtures and water was added and mixed for 2 min. For the first three mixes fresh properties were then measured. Finally, the concrete was remixed for 1 min.

In the pilot study the desired flowing consistency was achieved with a quite rich mix with only sand (0–8 mm) as aggregate, w/b = 0.40, paste volume = 47% and matrix volume (including all particles <0.125 mm) = 50% of volume, and using 1% water reducer by weight of cement. For the last part of the study, with three different pipe materials in the larger flow test set-up, leaner mixes were made with w/b = 0.50, paste volume = 36%, matrix volume = 40% and 25% of the sand replaced with 4-8 mm aggregate. In Mixes 1–4 with constant w/b the matrix quality was varied with viscosity modifying agent, silica fume and filler, while maintaining stability and flow-ability. The dosage of water reducer varied from 0.7 to 2% by weight of binder for uncoloured mixes and adding 0.5% to coloured mixes to compensate for loss of flow due to the pigments. Air void content of fresh concrete was assumed to be 2% for all mixes. For the first three mixes, workability was determined in terms of slump flow and T_{50} according to [15,27], and plastic viscosity and yield stress were measured with the BML ConTec viscometer [15,17,18,20].

Table 1 presents composition of mortars used in the flow experiments. Mixes 1–4 followed some pilot studies with a parallel plate viscometer with the actual concrete materials finer than 0.125 mm to obtain matrices with large variations of τ_0 and μ [28]. Properties of fresh concrete were determined for the pilot mixes and for Mix 1. For the rest of the mixes, only flow rates were determined. All mixes were stable with respect to segregation and bleeding. The concrete materials were: a granitic aggregate from Årdal Norway [29] consisting of 0-8 mm sand with 6.3–6.7% material finer than 0.125 mm and 0.8% absorption by mass, and 4–8 mm mixed natural/crushed material with 0.5% absorption by mass. The particle density was 2670 kg/m^3. In one mix, additional natural filler <0.125 mm of the same origin was added. The cement was a Norwegian manufactured Norcem Standard FA conforming to the designation CEM II 42.5 [30] with 20% interground low lime fly ash and density of 2950 kg/m^3. A dry Elkem micro silica grade 9400 with density 2200 kg/m^3 was used. The water reducer was a co-polymer from BASF; Glenium 151 with 15% solid content and density of 1000 kg/m^3. In addition, a polymeric stabilizer was used in Mix 2; SIKA 4R with 4.5% solid content and density of 1000 kg/m^3.

2.3. Pigments

In the pilot study, different colouring agents and pigments were investigated in terms of sharpness of interface between coloured and uncoloured concrete and effect on workability. Interface sharpness was observed by filling cube moulds halfway with uncoloured concrete, topping with coloured concrete, hardening for a few days before sawing and visual inspection. A brown iron oxide powder pigment (600 Ferroxon) was found to give best and sufficient sharpness at a dosage of 1.7% by mass of cement with relatively low effect on workability without

Table 1
Compositions of mortars and concrete (kg/m^3).

Mix colour	Pilot w/b = 0.40		1, w/b = 0.50		2, w/b = 0.50		3, w/b = 0.50		4, w/b = 0.50	
	Gray	Brown	Gray	Black	Gray	Black	Gray	Black	Gray	Black
Cement	631	629	442	438	429	426	397	394	418	415
SF	–	–	–	–	10.7	10.6	19.8	19.7	20.9	20.7
Free water	252	252	221	219	220	218	208	207	220	218
Sand	1360	1357	1219	1219	1219	1219	1219	1219	1219	1219
Coarse	–		406	406	406	406	406	406	406	406
Nat. filler	–	–	–	–	–	–	49.6	49.2	–	–
WRA	6.31	6.29	4.42	6.57	8.58	10.64	4.76	6.7	3.35	5.39
Stabilizer	–	–	–	–	4.29	4.26	–	–	–	–
Pigment	–	11	–	13.15	–	12.7	–	11.82	–	12.45
Density	2249	2255	2292	2302	2298	2307	2304	2313	2287	2297

additional water reducer. For the final four Mixes, with stronger colour boundary sharpness, a black iron oxide (612 Ferroxon) pigment in powder form was used at a dosage of 3% of cement. The particle densities of the two pigments were 4400 and 4500 kg/m^3 respectively. 3% black pigment affected workability and flow considerably compared to 1.7% brown pigment in the pilot mortars. For this reason, the dosage of water reducer was increased from 1 to 1.5% of cement for black mixes to reach similar flow as the gray mixes.

2.4. Mixtures and properties of fresh concrete

Table 2 presents the properties of fresh mixes showing that the two rich pilot mortars with w/b = 0.40 had similar T_{50}, slump flow and plastic viscosities, whereas the yield stress was increased by the colouring agent at constant dosage of water reducer. The leaner Mix 1 with w/b = 0.50 had higher flow in terms of reduced T_{50}, increased slump flow and reduced yield value. Plastic viscosity was similar for the three mixes. Due to the very busy test scheme, with fast mixing and filling of gray and coloured mortars, measurement of flow etc, only visual inspection of the stability of the rest of the mixes were made and found to be satisfactory.

3. Results and discussion

3.1. Flow profiles

Fig. 3 shows the sawn surfaces of hardened concrete after pipe flow tests of the pilot mix, illustrating how the flow profiles develop at increasing flow rate. Figs. 4–13 show photos of the sawn interfaces between gray and coloured concrete of Mixes 1–4 after hardening, as well as the back sides of the specimens showing the concrete surfaces towards the pipe wall. The pictures are manipulated to show both cut and wall surface.

The flow profiles were marked with black ink pen as seen in the photos, sometimes indicating a more or less abrupt stop towards the pipe wall. The marker pen did, however, sometimes cover a thin gray layer close to the wall, like that seen to the left of the ink marking in Fig. 4. This kind of layer corresponds to the thickness of the gray colour seen at the back side of the pipe. Looking closer at the highest flow of the vertical pipe (0.7 m/s in Fig. 3), a less coloured rim in the order of 1 mm wide is seen along both sides of the coloured concrete, indicating some sort of slip in this vertically downwards flowing concrete. At the lower angles, there were also possible effects of gravity in that the coloured concrete was seemingly pushing away the gray concrete more in the lower part than in the upper part, see the profiles at 15, 30 and 45° to the horizontal plane.

Table 2
Properties of fresh concrete.

Mix	Pilot Mix gray	Pilot Mix brown	Mix 1 gray
T_{50} (s)	2.3	2.4	0.5
Slump flow (mm)	645	645	760
τ_0 (Pa)	10	30	≈ 0
μ (Pa s)	8	9	9

An important feature of Figs. 3–13 is that in most cases flow profiles develop over the cross section. For the pilot mixes, this is a clear function of increasing flow rate, with plug at the lowest flow rate and an increasing variation of flow rate over the cross section at the highest flow rate. For Mixes 1–4, there is most plug tendency for the acryl pipe (Figs. 5 and 7) and steel pipe (Figs. 8 and 11), whereas for the rubber pipe there seems to be velocity profiles (Figs. 4, 9 and 12). Due to the short flow length of the coloured concrete, it is not likely that these are fully developed flow profiles.

3.2. Slip layers and flow profiles

The variation of flow velocity over the pipe cross section in Figs. 4–13 was described from maximum observed length of the coloured concrete (upper photo) and the length of the coloured slip interface (lower photo). The length of the maximum observable flow variation over the test period, L (m), can be determined, Eq. (3):

$$L = (\max - slip) \tag{3}$$

Here, max (m) is determined from the upper and slip (m) from the lower photos. The value of max = distance from the left end of the specimen to the tip of the coloured flow profile at the right. Slip layers in the lower photos of Figs. 4-13 can be defined as coloured concrete surface towards the pipe, i.e. where the coloured concrete has been in movement at the pipe wall. The value of slip = distance from the left to the point where the surface colour changes from black to gray in the lower photos. The points of colour change on the lower photos are less

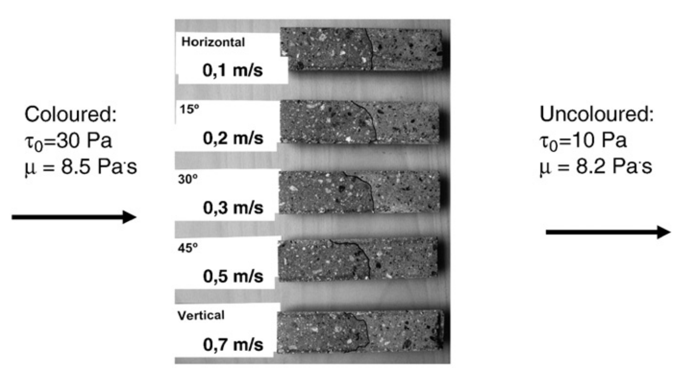

Fig. 3. Flow profiles Pilot mix with w/b = 0.40 in 30 mm diameter PVC pipe.

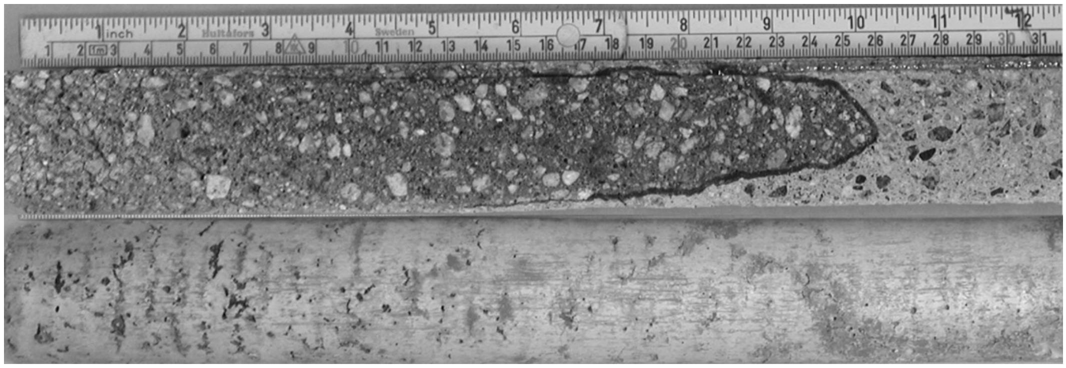

Fig. 4. Flow profiles (upper) and pipe wall surface (lower) Mix 1 — rubber, $v = 0.2$ m/s.

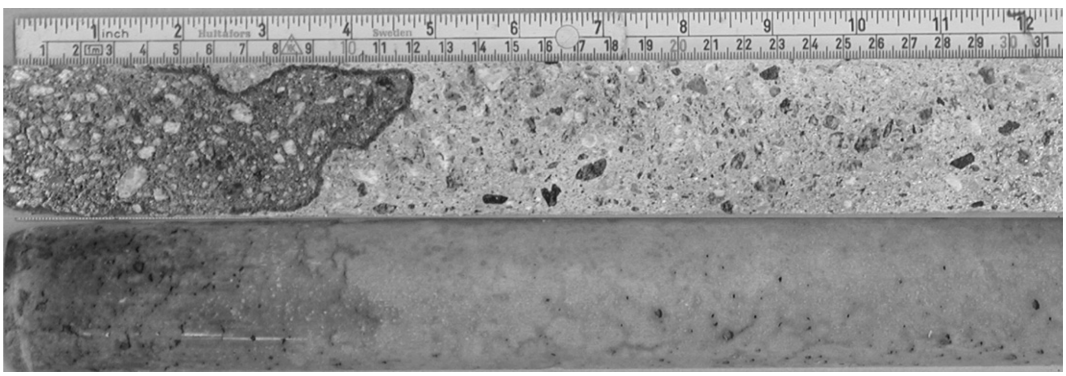

Fig. 5. Flow profiles (upper) and pipe wall surface (lower) Mix 1 — acryl, $v = 0.4$ m/s.

clearly defined than in the upper photos, but indicate velocities at the wall and thus the boundary conditions. The values of slip were therefore taken as halfway between completely coloured and completely gray when observing from left to right. The results are given in Table 3 and indicate that the rubber pipe has large *L* whereas the low friction acryl has low *L*. For steel, the observations and estimates seem more uncertain. For some of the shortest flow profiles, like for Mix 3 in acryl pipe and Mix 4 in steel pipe, the flow profile is probably very close to complete plug flow. Considering the flow rates (0.23 and 0.26 m/s, which are relatively high compared to the lowest flow rates, see Table 4), the observations indicate that slip- (or boundary) conditions and flow profile may be linked to each other or interrelated in some way, with long slip giving low variation of flow over the cross section and vice versa. Care was taken during observation and photographing to use equal aperture, exposure time, light and background. However, due to the subjective nature of the method of observation and that the surfaces were slightly moistened to see colour differences better, the estimates in Table 3 are still a bit uncertain. Colour towards the pipe surface entered a surface already primed by the gray concrete. These observations therefore reflect differences in boundary flow, even though over very short flow distances. In real pumping, the conditions will differ due to higher pressure and flow rate, probably affecting slip layers and rheology.

3.3. Flow rates

Fig. 14 shows accumulated mass of concrete vs. time for concrete Mixes 1–4 and the three different pipes. Flow rates were calculated with the individual concrete densities and pipe cross sections and are given in Table 4. The correlations to linear curves are very good and allow comparison of the different materials. The accuracy of the simple measurements on the pilot mixes with watch and beaker are

Fig. 6. Flow profiles (upper) and pipe wall surface (lower) Mix 1 — steel, $v = 0.3$ m/s.

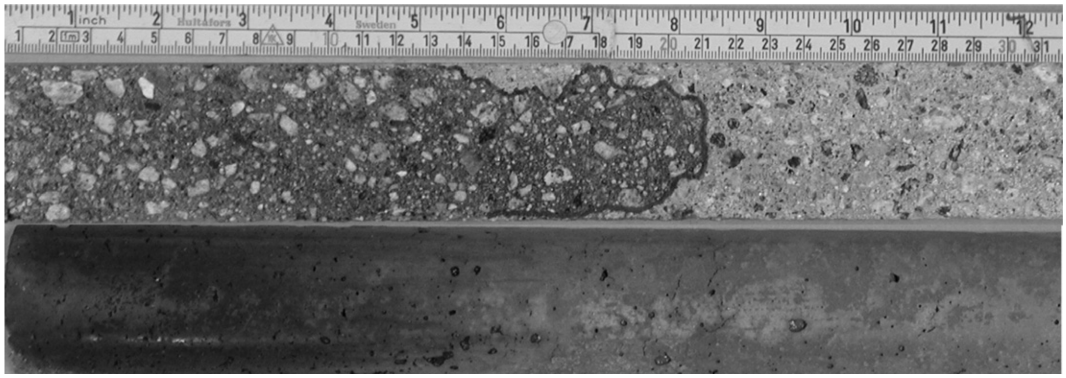

Fig. 7. Flow profiles (upper) and pipe wall surface (lower) Mix 2 — acryl, $v = 0.2$ m/s.

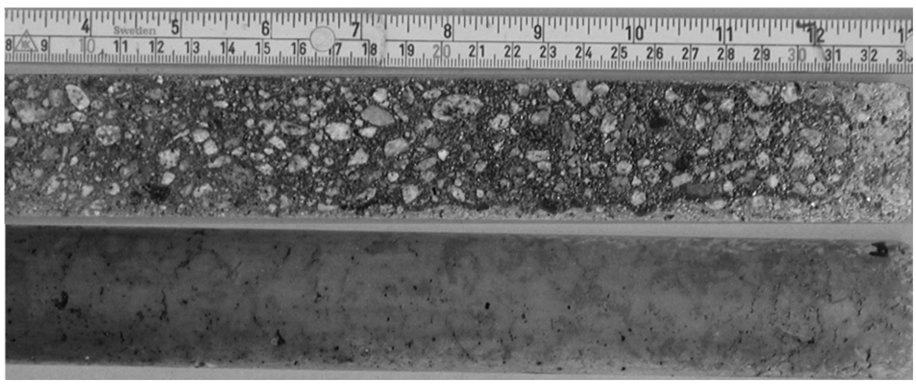

Fig. 8. Flow profiles (upper) and pipe wall surface (lower) Mix 2 — steel, $v = 0.1$ m/s. (The hardened sample from Mix 2–rubber pipe–was damaged and not fit for further testing.)

Fig. 9. Flow profiles (upper) and pipe wall surface (lower) Mix 3 — rubber, $v = 0.2$ m/s.

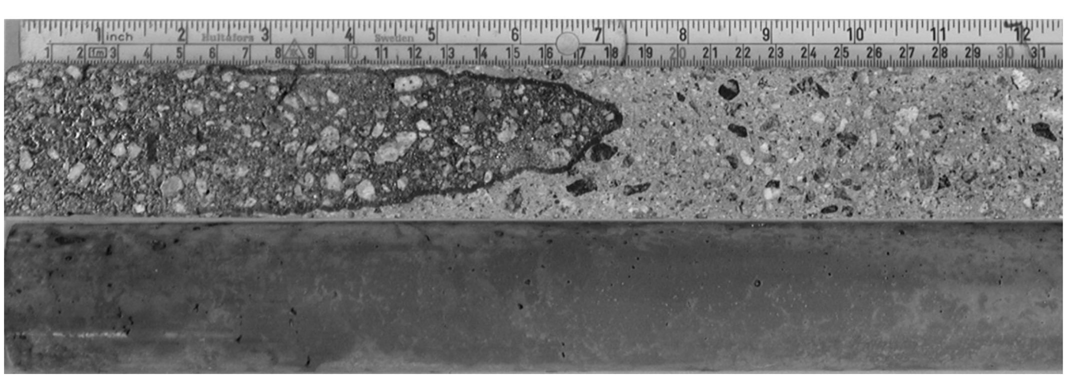

Fig. 10. Flow profiles (upper) and pipe wall surface (lower) Mix 3 — acryl, $v = 0.3$ m/s. The hardened sample from Mix 3–steel pipe–was damaged and not fit for further testing.

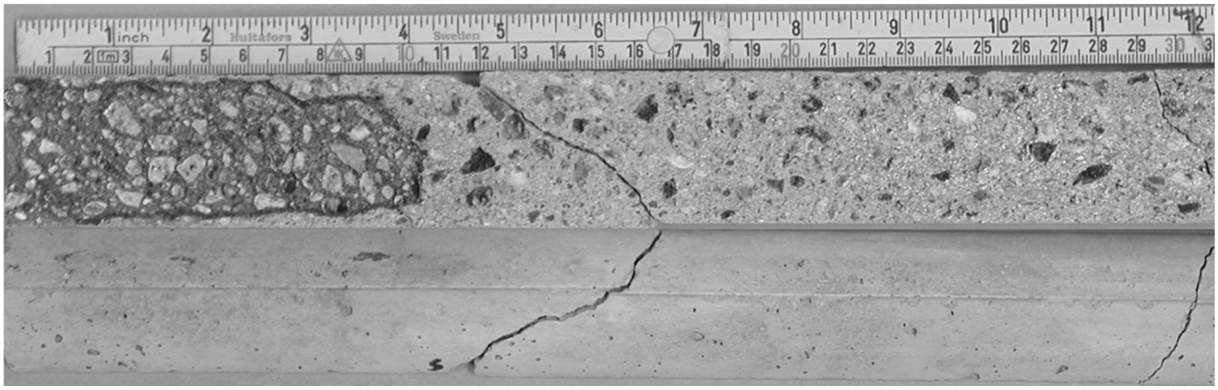

Fig. 11. Flow profiles (upper) and pipe wall surface (lower) Mix 4 — steel, $v = 0.2$ m/s.

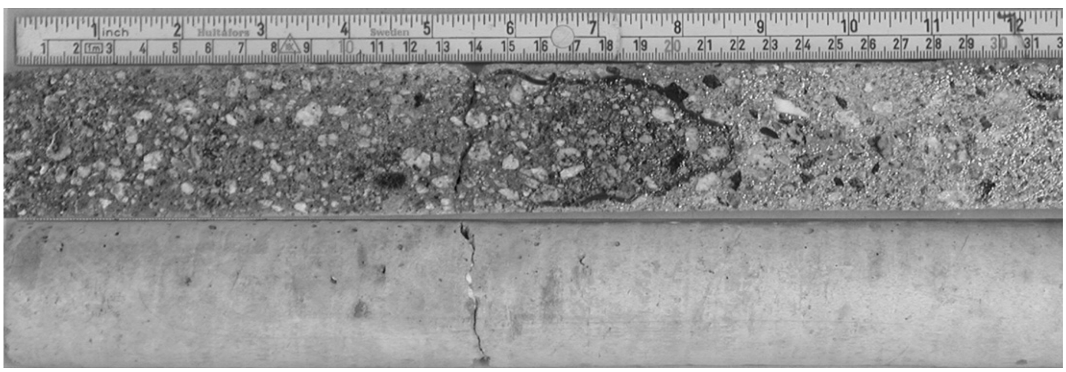

Fig. 12. Flow profiles (upper) and pipe wall surface (lower) Mix 4 — rubber, $v = 0.3$ m/s.

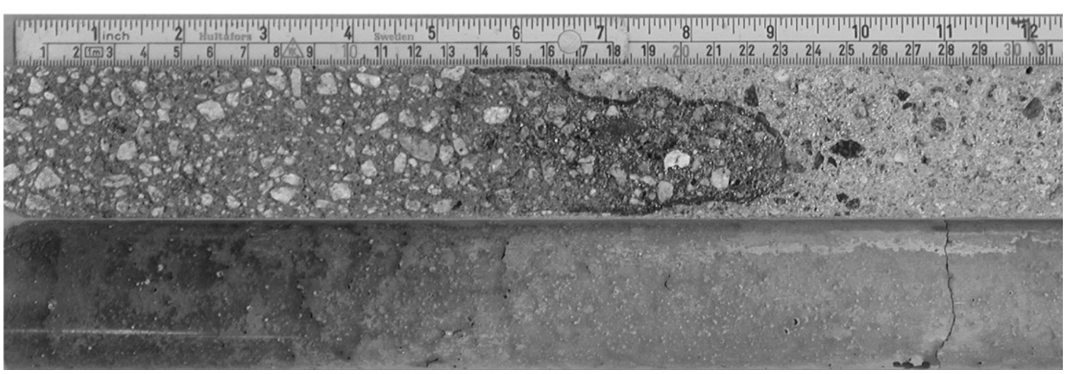

Fig. 13. Flow profiles (upper) and pipe wall surface (lower) Mix 4 — acryl, $v = 0.3$ m/s.

low compared to Mixes 1–4. Due to the low flow distances and low pressure in the pipes, the flow probably depends at least as much on friction due to pipe surface roughness as on concrete rheology.

Table 3
Estimated length of flow profile (L).

Mix	Acryl	Rubber	Steel
	$L = (\max - \text{slip})$ [cm]		
1	8	26	19
2	9	[a]	18
3	2	28	[a]
4	7	22	1
L mean	6	25	13
S.D.	3	3	10

[a] No observations.

From Table 4 we see that flow increases with increasing angle of the 30 mm pipe, as expected. Comparing pipes in Fig. 14 and Table 4 we see that acryl always has higher flow. Furthermore, Mix 2 with the viscosity modifying agent has the lowest flow rate of the four mixes for all three pipe materials. The average flow is $v = 0.29$ m/s in the acrylic pipe and $v = 0.21$ m/s in the rubber pipe. (Unfortunately, the steel pipe had a bit lower diameter giving a size effect, disturbing comparison of steel with acryl and rubber). Furthermore, the flow of the “sticky” Mixes 3 and 4 with high dosages of silica fume are affected less by varying pipe material than the other two mixes, showing only a moderately higher flow in the acrylic pipe than in the rubber pipe. Possibly, the effect of pipe material is strongest for the reference Mix 1 without any stabilizer, additional filler or silica fume and for Mix 2 with stabilizer and low silica dosage. By comparing the four concrete mixes within each of the three pipe materials, we see that the mixes

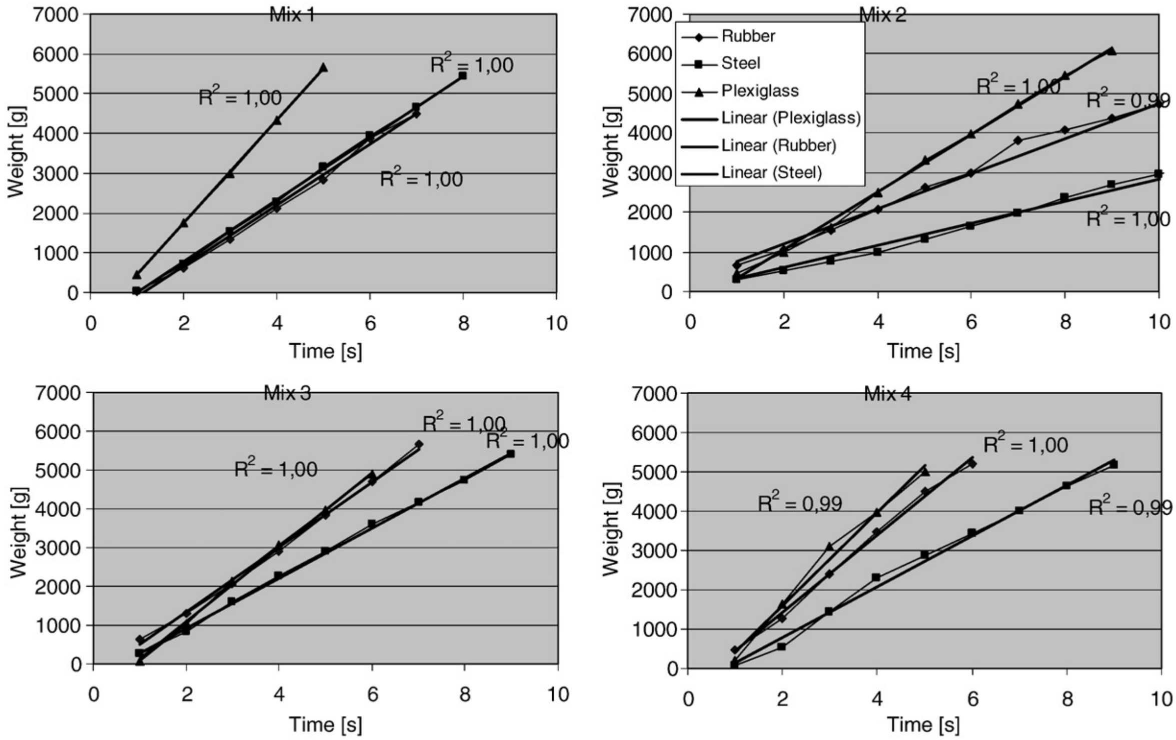

Fig. 14. Cumulated mass vs. time during concrete flow.

are ranked equally in the acrylic and the steel pipe with Mix 1 giving highest and Mix 2 giving lowest flow. For the rubber pipe the situation is different, with the sticky, high dosage silica fume, Mixes 3 and 4 are giving the highest flow. It is therefore possible that the effect of pipe material on concrete flow depends on concrete composition.

3.4. Amount of concrete sticking to pipe surface — SEM observations of pipe surfaces

To quantify the adhesion or friction between concrete and pipe and assess the surface roughness, measurements were made of the amount of concrete sticking to the pipe after emptying, and some SEM observations were made on pipe surfaces. A clean and dry piece of pipe was weighed, filled with concrete Mix 1 while held in vertical position on the floor and then emptied by lifting vertically like a slump cone and weighed again. The experiment was done 3 times for each pipe material giving on average 0.36, 0.84 and 0.64 kg/m^2 fresh concrete (mainly matrix) stuck to the acryl, rubber and steel pipes, respectively (coefficient of variation 23–40%). The ranking is equal to that of the flow rate for this mix in the 3 pipe materials, supporting that friction is dominant in this short time flow study. The amount stuck to the pipe wall has 0.1–0.3 mm average thickness, consuming 3–7 vol.% of the matrix (= paste and filler) in the concrete filling the pipe, which is a significant loss at first time flowing. Fig. 15 shows typical SEM images taken of the pipe surfaces. The rubber surfaces have a number of bumps in the order of 20–40 μm in diameter, whereas the steel has flakier and flat uneven areas of around 100 μm in size. No surface texture could be seen on the acrylic pipe at this magnification, illustrating the importance of roughness and friction. In addition to the effect of roughness, the soft rubber pipe will absorb energy from impacts reducing particle movement along the pipe surface.

3.5. Slip layers and coarse particles

Slip layers may develop due to radial migration of coarse particles from zones with high shear to zones with low shear [3,31,32]. The tendency should increase with increasing rate of shear near the wall. Furthermore, due to the wall effect between aggregate particles and pipe surface there is locally increased matrix volume in a zone of thickness half the maximum aggregate size $d/2$ (m) from the wall [33]. The volume of the affected zone due to the wall effect, $V_{\mathrm{aff,\,p}}$ (m^3) relates to the concrete volume in a pipe of diameter D (m) according to Eq. (4) [33]:

$$\frac{V_{aff,p}}{V} = 1-\left[\frac{(D-d)^2}{D^2}\right]. \tag{4}$$

For our experiments these theoretically affected volume fractions are quite high; 0.46 and 0.32 for 30 and 45 mm pipes, respectively.

Table 4
Measured flow, v [m/s].

Pipe diam./mat.	30 mm PVC (Pilot)					45 mm		40 mm	
Conc./tilt/pipe mat.	hor.	15°	30°	45°	vert.	Acrylic 45°	Rubber 45°	Steel 45°	Acr./Rubb.
Pilot, w/c = 0.4	0.1	0. 2	0.3	0.5	0.7				
Mix 1, w/c = 0.5						0.36	0.21	0.27	1.7
Mix 2, w/c = 0.5						0.20	0.12	0.10	1.6
Mix 3, w/c = 0.5						0.26	0.23	0.22	1.1
Mix 4, w/c = 0.5						0.33	0.27	0.23	1.2

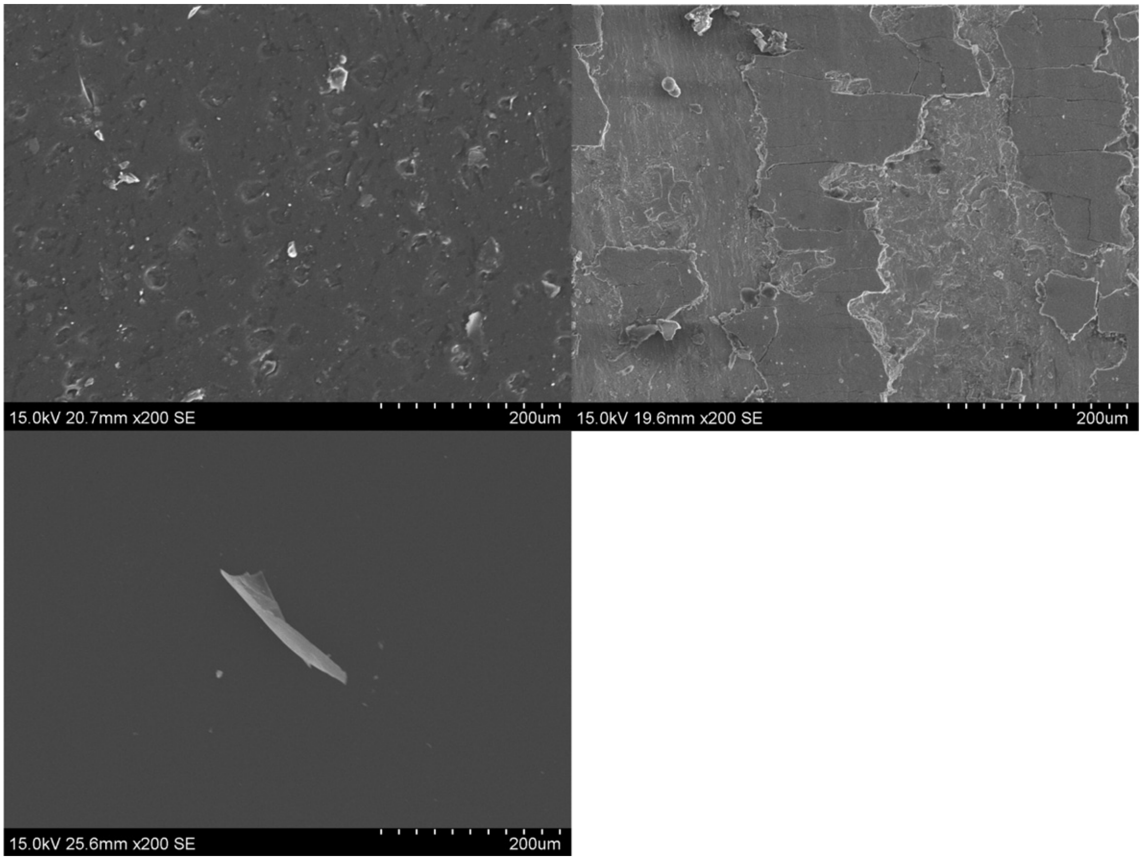

Fig. 15. SEM images of the roughest rubber surface and steel (upper left and right) and the smooth acryl pipe (lower). Some fragments seen from drying cloth.

Since the volume fraction of coarse aggregate affects rheology [32], the concrete close to the wall could have different flow properties from the concrete in the central portion of the pipe. The corresponding wall affected volume fraction in our concentric BML-viscometer can easily be determined, Eq. (5):

$$\frac{V_{aff,B}}{V} = \frac{12d}{D}. \tag{5}$$

For our viscometer with outer diameter $D = 400$ mm and core diameter $D/2 = 200$ mm $(V_{aff,B}/V) = 0.24$. The concrete in the BML is thus possibly somewhat less affected by the wall than the concrete in the pipe experiments. An effort was made to measure coarse aggregate content with image analysis [34]. However, no evidence was found of increased aggregate content towards the centre axis of the pipe. Possibly a larger specimen is needed to detect the wall effect. Furthermore, the coloured concrete should flow over a longer distance and/or at higher velocity to imitate the conditions of segregation under shear.

4. Conclusions

Experiments with coloured fresh concrete flowing after ordinary (gray) concrete were made to observe the flow conditions in various pipes. Slip layers and variation of flow rate over the pipe cross section were observed as colouring on hardened surfaces towards the pipe, and on sawn surfaces along the central pipe axis. Rubber pipes showed long flow profiles with low velocity at the wall (no/little slip), whereas the acryl pipes showed more plug flow with long slip layers and less profile or variation of flow rate over the cross section. It seems that slip- (or boundary) conditions and flow profile may be interrelated in some way, with long slip giving low variation of flow over the cross section and vice verse. The ranking of flow rate for the investigated mixes was different between rubber and the two other pipe materials. Highest flow rate observed in the rubber pipe occurred for the high silica fume mix, whereas the reference mix without silica fume had highest flow in acryl- and steel pipes. Due to the short flow lengths and low pressure, pipe wall roughness and friction may be more dominant in these experiments than in high pressure pumping where pressurized bleeding, segregation under shear and other effects may affect both slip layers and rheology of the concrete.

Acknowledgments

Thanks to Ove Loraas and Gøran Loraas at the concrete laboratory of The Norwegian University of Science and Technology, Department of Structural Engineering for their valuable laboratory assistance. Furthermore, thanks to Dr. Einar Aassved Hansen and Dr. Hedda Vikan at Sintef for support. The investigation was a part of COIN Task Group 2. COIN (COncrete INnovation centre) started in January 2007 as a Centre for Research based Innovation (CRI) within concrete technology at SINTEF Building and Infrastructure and NTNU Dept of Structural Engineering with industrial partners: Aker Solutions, Norcem Heidelberg, Borregaard, Maxit M-Tec Weber St.Gobain, Skanska, Rescon Mapei, UNICON, Veidekke, Consolis and the Norwegian Road directory. Thanks to Ph.D. Siaw Foon Lee for assistance with the SEM and for performing the image analysis of aggregate concentration across the pipes. Finally, thanks to the reviewers for helpful critics.

References

[1] T. Cooke, Concrete pumping and spraying — a practical guide, Th.Telford, Lon, 1990 251 pp.
[2] D. Kaplan, Pompage des bétons, Thèse de doctorat ENPC/ LCPC, Paris, 2001 228 pp.
[3] L.H. Thrane, Form Filling with SCC, Concrete Centre DTI/DTU, Denmark, 2007 269 pp.
[4] N. Roussel, Rheology of fresh concrete: from measurements to predictions of casting processes, Materials and Structures (49) (2007) 1001–1012.

[5] A. Gram, S. Mechtcherine, K. Schwabe, K. Krentzer, J. Silfwerbrand, Modelling and simulation of SCC flow, Presentation SCC2008, ACBM, Chicago, 2008 51 pp.
[6] J.E. Wallevik, Minimizing end-effects in the coaxial cylinders viscometer: viscoplastic flow inside the ConTech BML Viscometer 3, J.Non-New Fl Mech 155 (2008) 116–123.
[7] ACI Comm.304 (1998) Placing concrete by pumping meth. ACI 304.2R-96, 2. Print 25 pp.
[8] M. Jolin, F. Chapdelaine, D. Burns, F. Gagnon, D. Baupré, Pumping concrete; a fundamental and practical approach, presentation Shotcrete for underground support X Sept.12-16/ Universitè Laval (2006), 2006 9 pp.
[9] M. Rössig, Fördern von Frischbeton, insbesondere von Leichtbeton, durch Rohrleitungen, Dr.diss, RWTH, Westdeutscher Verlag, ISBN 3-531-02456-6, 1974 132 pp. + 92 pp. fig/tab.
[10] G.H. Tattersall, P.F.G. Banfill, The rheology of fresh concrete, Pitman Books Ltd., London, 1983 356 pp.
[11] Jacobsen S., Mork J.-H., Lee S.F, Haugan L. (2008) Pumping of concrete and mortar – State of the art, COIN Project Report no. 5, ISBN 978-82-536-1069-6, Norw Univ of Sc and Tech-SINTEF 42 pp., 5 app.
[12] A.N. Ede, The resistance of concrete pumped through pipelines, Magazine of Concrete Research (1957) 129–140 November.
[13] D. Browne Roger, B. Bamforth Phillip, Tests to establish concrete pumpability, ACI Journal (1977) 193–203 May 1977.
[14] Hansen J.K.B.(1988) Characterisation of concrete pumpability using the two-point apparatus, HPC Materials Dev rep 3.2, report no Sintef STF 65 F89046 (In Norw.) 45 pp.
[15] Bartos R.J.M, Sonebi M and Tamimi A.K.(2002) Workability and Rheology of Fresh Concrete: Compendium of Tests, Report of RILEM TC 145-WSM, RILEM Publications, 127 pp.
[16] C Hu, F. De Larrard, T. Sedran, A new rheometer for high performance concrete, 4th Int Symp on HS/HPC, LCPC/Presses de ENPC, Paris, 1996, pp. 179–186.
[17] Wallevik O.(1990) Rheology of fresh concrete and utilization on concrete with and without silica fume, Dr.ing dissertation 1990:45 Norw.Un.Sc.&Tech, 182 pp. (In Norw.).
[18] O. Wallevik, O.E. Gjørv, Development of a coaxial cylinders viscosimeter for fresh concrete, Proc RILEM Int conference on properties of fresh concrete, 1990, pp. 213–224.
[19] J-H. Mork, A presentation of the BML-viscometer, in: P.J.M. Bartos, et al., (Eds.), Production methods and workability of concrete, RILEM Proc., 32, 1996, pp. 369–376.
[20] J.E. Wallevik, Rheology of particle suspensions. Fresh concrete, mortar and cement paste with various types of lignosulfonates, 2003 Dr.ing 2003:18 Norw.Un.Sc. &Tech, 397 pp.
[21] V. Vassiliev, Concrete flow regime in pipes, 1953 Originally published in Russian, cited in the PhD of Denis Kaplan 2001 pp. 33-34.
[22] A. Nanayakkara, D. Gunatilaka, K. Ozawa, K. Maekawa, Mathematical modelling of deformation for fresh concrete in pumping, Univ of Tokyo, 1988, pp. 819–824, Paper 1146.
[23] D. Kaplan, F. deLarrard, T. Sedran, Avoidance of blockages in concrete pumping process, ACI Materials Journal 102 (3) (2005) 183–191.
[24] Mork J.H.(1994) Effect of gypsum-hemi hydrate ratio of cement on rheology of fresh concrete, dr.ing dissertation (In Norwegian) NTH 1994:04, Trondheim, Norway, 286 pp.
[25] E. Mørtsell, S. Smeplass, T.A. Hammer, M. Maage, Flowcyl — how to determine the flow properties of the matrix phase of high performance concrete, 4th Int Symp on HS/HPC, LCPC/Presses de ENPC, Paris, Paris, 1996, pp. 26–268.
[26] D Feys, B. Calie, R. Verhoeven, G. De Schutter, Evaluation of gravitational flow tests with SCC in pipes as a forecast for pumping pressures, 5th Int. symp. on SCC, Rilem PRO54 ISBN 978-2-35158-047-9, vol.1, 2007, pp. 515–520.
[27] European guidelines for self compacting concrete, Specification, production and use, 2005 ERMCO/CEMBUREAU/EFNARC, 63 pp.
[28] L. Haugan, Unpublished results, Sintef-NTNU, Norway, 2009.
[29] NS3099 Norwegian Standard NS3099, Reference Concrete ICS 91.100.30 (1999) 4pp.
[30] NS-EN 197-1:2000, Cement part 1: Composition, specifications and conformity criteria for common cements, standard Norge ICS 91.100.10;2005:39 pp.
[31] M. Haist, H.S. Müller, Optimization of the pumpability of self-compacting light weight concrete, Proc SCC 2005 ACBM, NWU, Evanston, 2005, 6 pp.
[32] F. Mahaut, S. Mokéddem, X. Chateau, N. Roussel, G. Ovarlez, Effect of coarse particle volume fraction on the yield stress and thixotropy of cementitious materials, Cement and concrete research 38 (11) (2008) 1276–1285.
[33] T. Sedran, F. DeLarrard, Mix design of Self Compacting Concrete (SCC), in: PJM Bartos, et al., (Eds.), Production methods and workability of concrete, RILEM Proc., 32, 1996, pp. 439–450.
[34] Lee S.F., Monsøy A., Lein H.L., Jacobsen S. (2009) paper submitted to Cement and Concrete Research.